Applied Mathematical Modelling 46 (2017) 365–381

Contents lists available at ScienceDirect

Applied Mathematical Modelling

journal homepage: www.elsevier.com/locate/apm

Mathematical modeling and simulation of the earth's magnetic field: A comparative study of the models on the spacecraft attitude control application

M. Navabi*, M. Barati

New Technologies Engineering Faculty, Shahid Beheshti University, GC, Tehran, Iran

ARTICLE INFO

Article history:
Received 2 June 2015
Revised 4 August 2016
Accepted 16 January 2017
Available online 19 January 2017

Keywords:
Earth's magnetic field models
Spacecraft attitude control
Linear and nonlinear transformation
Orbital frame
Body frame

ABSTRACT

In this paper, the Earth's magnetic field models which are widely used in spacecraft attitude control applications are modeled and extensively compared with a reference model. The reference model is obtained utilizing coefficients from the last generation of International Geomagnetic Reference Field (IGRF-12). The validity of this model is verified with the World Magnetic Model (WMM) in terms of intensity and direction of the field. The reference model is then used to evaluate lower-order and approximating models while the influence of effective parameters such as expansion order of modeling, orbit height, inclination, latitude and longitude on accuracy of modeling is investigated. The simulation results for several scenarios are presented and discussed. The linear and nonlinear transformations of the models from orbital frame to spacecraft body frame are compared for a wide range of attitude angles in order to investigate the sensibility and validity of linear transformation. Simulation of a spacecraft attitude control maneuver is performed to demonstrate the importance of the accuracy of the magnetic field model which is implemented in the attitude control system. The results indicated a meaningful increase in control effort when a simplified model was used. This research was aimed to investigate the borders of different geomagnetic field models and transformations for spacecraft attitude control applications. The presented results may lead to a proper choice of the Earth's magnetic field model based on the space mission requirements.

1. Introduction

In recent decades, there has been a growing interest in employing satellites in low Earth orbits (LEO). Not only a wide range of newly defined scientific objectives can be achieved by LEO satellites, but also significant mission cost reductions in such orbits have brought a great attention to them. This has led scientists to perform deeper investigations on all aspects of LEO missions and also to make revisions on topics that were quite known before.

An essential part of spacecraft for operation and achievement of mission goals is attitude control system (ACS). Extensive research has been done in the literature to improve the functionality of ACS in terms of accuracy and energy saving [1–8]. One of the conventional methods in spacecraft attitude control which is proved to be very effective and practical is the use of the Earth's magnetic field [4–11]. In this approach, a part or the whole required actuation is achieved by a set

* Corresponding author.
E-mail address: civil.space.edu@gmail.com (M. Navabi).

http://dx.doi.org/10.1016/j.apm.2017.01.040
0307-904X/

of electromagnetic coils producing the control torque in interaction with geomagnetic field [9–12]. Exploiting the Earth's magnetic field is especially applicable for LEO satellites since the field in such orbits has enough intensity to be used for attitude control. Furthermore, using magnetic coils is considerably less costly and less complex than other actuation methods used in ACS such as reaction wheels or thrusters [9,13]. In overall, it is evident that using geomagnetic field for satellite attitude control–alone or in cooperation with other methods– is widely considered for LEO missions. This is where the importance of accurately modeling the Earth's magnetic field becomes bold.

The Earth magnetic field can be analytically represented by a series of spherical harmonics including Gaussian coefficients and associated Legendre polynomials [14]. Hence, there are expansion models with different degrees which their accuracy depends on where they are truncated and how accurate the Gaussian coefficients of the series are measured. A first degree truncation constitutes a rather simple set of expressions named Dipole Model which models the Earth's magnetic field as a dipole. There are also models which make use of simplifying assumptions on dipole model to make them more convenient to use such as Centered Dipole Model and Simplified Dipole Model which will be further explained in Section 2. Second, third and fourth degree expansions are called Quadrupole, Octupole and Sedecimupole Models respectively. Expanding the harmonics to higher degrees increases the accuracy of modeling. However, the quality of Gaussian coefficients measurements confines us to the 13th degree according to the most recent generation of IGRF (IGRF-12) [15]. The 13th degree model which is valid till 2020 when the next version will be released is one of the most accurate and reliable models of the geomagnetic field currently available and is named Reference Model in this context.

The main purpose of this study is to give an assessment on various Earth's magnetic field models and reveal their limits and border of validity utilizing mathematical modeling and simulation techniques. To this end, a comprehensive evaluation of the Earth's magnetic field models is carried out considering the effects of important parameters such as expansion order of modeling and mission specifications such as orbital altitude and inclination. Next, the problem of transforming the geomagnetic field model from orbital frame to spacecraft body frame is considered. This transformation could be performed with either a linear method or a nonlinear one. The small angle assumption in spacecraft attitude control problem is shown to be a challenging topic in the literature [16]. There, we investigate how this assumption affects the results of geomagnetic filed model transformation.

In the first part of this paper, mathematics of geomagnetic field modeling required for generating the software codes used in simulations are described. Within this section, the selected models are introduced and transformations for describing the magnetic field in required coordinate systems are presented. Next, verification results for our reference model based on 12th version of IGRF are presented. The paper follows with the results of simulations and comparisons of the models for different scenarios. Effects of important factors such as orbital inclination, altitude and expansion order are depicted and discussed. Next, simulations are performed to evaluate the linear transformation of magnetic field from orbital frame to spacecraft body frame regarding various attitude angles. A simulation case study of an attitude control maneuver is considered for illustrating the importance of geomagnetic field model selection. Eventually, the conclusion of this paper is presented to briefly express the outcomes of this study.

2. Mathematical modeling of the earth's magnetic field

A rigid spacecraft can be described as a system of particles that their relative distances are fixed during the time. Attitude equation of such spacecraft is as follows [17].

$$\mathbf{T} = \dot{\mathbf{h}}_I = \dot{\mathbf{h}}_B + \omega \times \mathbf{h}_B, \tag{1}$$

where $\mathbf{T}$ denotes the external moments vector, $\mathbf{h}$ is the angular momentum vector, and $\boldsymbol{\omega}$ shows the angular velocity vector, the subscripts I and B refer to the inertial frame and body frame respectively. In derivation of the spacecraft attitude equations, external moments are shown as the sum of disturbance ($\mathbf{T_d}$) and control ($\mathbf{T_c}$) torques: $\mathbf{T} = \mathbf{T_c} + \mathbf{T_d}$ and the total angular momentum as the sum of rigid body ($\mathbf{h}$) and momentum exchange devices ($\mathbf{h}_w$) angular momentum: $\mathbf{h}_B = \mathbf{h} + \mathbf{h}_w$.

The magnetic control torque ($\mathbf{T}_c = \mathbf{T}_{mag}$) is produced by cross product of the magnetic dipole ($\mathbf{m}$) and the Earth's magnetic field vector ($\mathbf{B}$).

$$\mathbf{T}_c = \mathbf{T}_{mag} = \mathbf{m} \times \mathbf{B}. \tag{2}$$

The Earth's magnetic field, $\mathbf{B}$, can be described as the negative gradient of a scalar potential function, V.

$$\mathbf{B} = -\nabla V. \tag{3}$$

The potential function, V, can be represented by a series of spherical harmonics [14]:

$$V(r, \phi, \theta) = R_e \sum_{n=1}^{N} \left(\frac{R_e}{r}\right)^{n+1} \sum_{m=0}^{n} [g_n^m \cos(m\phi) + h_n^m \sin(m\phi)] P_n^m(\theta), \tag{4}$$

where R_e is the equatorial radius of the Earth, g_n^m and h_n^m are Gaussian coefficients, r, φ and θ are the geocentric distance, co-elevation and East longitude from Greenwich respectively that can define any point in the space.

The set of Gaussian coefficients for use in the analytical models describing the Earth's magnetic field are called the International Geomagnetic Reference Field (IGRF). Every five years, a group from the International Association of Geomagnetism

and Aeronomy (IAGA) examines the high-quality and globally distributed observations of geomagnetic field and produce new coefficients in unit of nanotesla (nT). In the last generation, IGRF-12 has taken advantage of a comprehensive set of observations including satellite measurements from the CHAMP, Ørsted and SAC–C missions [18], and international observatory measurements. Because the geomagnetic field is time-varying, the IGRF model also includes the so called secular variation (SV) coefficients such that for the five years after the most recent epoch, the SV can be used for forward linear extrapolation. The IGRF-12 model which is used in this study is the 12th generation model giving the 2010 spherical harmonic coefficients together with their respective secular variation terms to calculate the coefficients for the next five years [15].

Because of the conservative nature of the magnetic field ($\nabla \times B = 0$), the Earth magnetic field in spherical coordinates is obtained by the gradient of the potential function in Eq. (4), as following.

$$\begin{aligned} B_r &= -\frac{\partial V}{\partial r} = \sum_{n=1}^{N}\left(\frac{R_e}{r}\right)^{n+2}(n+1)\sum_{m=0}^{n}[g_n^m\cos(m\phi)+h_n^m\sin(m\phi)]P_n^m(\theta) \\ B_\theta &= -\frac{1}{r}\frac{\partial V}{\partial \theta} = -\sum_{n=1}^{N}\left(\frac{R_e}{r}\right)^{n+2}\sum_{m=0}^{n}[g_n^m\cos(m\phi)+h_n^m\sin(m\phi)]\frac{\partial P_n^m(\theta)}{\partial\theta} \\ B_\phi &= \frac{-1}{r\sin\theta}\frac{\partial V}{\partial \phi} = -\frac{1}{\sin(\theta)}\sum_{n=1}^{N}\left(\frac{R_e}{r}\right)^{n+2}\sum_{m=0}^{n}[-mg_n^m\sin(m\phi)+mh_n^m\cos(m\phi)]P_n^m(\theta), \end{aligned} \tag{5}$$

where $P_n^m(\theta)$ and $\frac{\partial P_n^m(\theta)}{\partial\theta}$ are associated Lagrange functions and their derivatives.

The recursive formulas for the Gaussian normalized associated Legendre polynomials and their derivatives are as follows.

$$\begin{aligned} P^{0,0} &= 1 \\ P^{n,n} &= \sin\theta P^{n-1,n-1} \\ P^{n,m} &= \cos\theta P^{n-1,m} - K^{n,m}P^{n-2,m} \\ K^{n,m} &= 0 \qquad n = 1 \\ K^{n,m} &= \frac{(n-1)^2-m^2}{(2n-1)(2n-3)} \qquad n > 1 \end{aligned} \tag{6}$$

$$\begin{aligned} \frac{\partial P^{0,0}}{\partial\theta} &= 0 \\ \frac{\partial P^{n,n}}{\partial\theta} &= \sin\theta\frac{\partial P^{n-1,n-1}}{\partial\theta} + \cos\theta P^{n-1,n-1} \\ \frac{\partial P^{n,m}}{\partial\theta} &= \cos\theta\frac{\partial P^{n-1,m}}{\partial\theta} - \sin\theta P^{n-1,m} - K^{n,m}\frac{\partial P^{n-2,m}}{\partial\theta}. \end{aligned} \tag{7}$$

Since associated Legendre polynomial ($P_{n,m}$) is displayed in the Gaussian normalized form ($P^{n,m}$), the $S_{n,m}$ is used to calculate the Gaussian normalized form of Gaussian coefficients ($g^{n,m}$, $h^{n,m}$) as Eq. (8).

$$S_{n.m} = \left[\frac{(2-\delta_m^0)(n-m)!}{(n+m)!}\right]^{1/2}\frac{(2n-1)!}{(n-m)!}. \tag{8}$$

The Kronecker delta is defined as $\delta_i^j = 1$ if $i = j$ and $\delta_i^j = 0$ otherwise. Using mathematical induction, it is possible to derive a recursion relation for $S_{n,m}$ as Eq. (9).

$$\begin{aligned} S_{0,0} &= 1 \\ S_{n,0} &= S_{n-1,0}\left(\frac{2n-1}{n}\right) \qquad n \geq 1 \\ S_{n,m} &= S_{n,m-1}\sqrt{\frac{(n-m+1)(\delta_m^1+1)}{n+m}} \qquad m \geq 1. \end{aligned} \tag{9}$$

$S_{n,m}$ is independent of r, φ and θ so it must be calculated only once. We define the normalized form of Gaussian coefficients as Eq. (10).

$$\begin{aligned} g^{n,m} &\equiv S_{n,m}g_n^m. \\ h^{n,m} &\equiv S_{n,m}h_n^m \end{aligned} \tag{10}$$

Obtaining the coefficients for the next five years from epoch requires using the predictive secular variation terms as mentioned earlier. This could be done according to the following linear expression.

$$g^{n,m}(t) = g^{n,m}(T_0) + \dot{g}^{n,m}(T_0)(t - T_0),$$
$$h^{n,m}(t) = h^{n,m}(T_0) + \dot{h}^{n,m}(T_0)(t - T_0) \tag{11}$$

where t is the time of interest in units of year and T_0 is the epoch preceding t. The average first time derivatives $\dot{g}_n^m$ and $\dot{h}_n^m$ denote the mentioned secular variations terms (SV) given in units of nTyr^{-1}.

Using above relations, the Earth's magnetic field is calculated as follows.

$$B_r = \sum_{n=1}^{N}\left(\frac{R_e}{r}\right)^{n+2}(n+1)\sum_{m=0}^{n}[g^{n,m}\cos(m\phi) + h^{n,m}\sin(m\phi)]P^{n,m}(\theta)$$
$$B_\theta = -\sum_{n=1}^{N}\left(\frac{R_e}{r}\right)^{n+2}\sum_{m=0}^{n}[g^{n,m}\cos(m\phi) + h^{n,m}\sin(m\phi)]\frac{\partial P^{n,m}(\theta)}{\partial\theta}$$
$$B_\phi = -\frac{1}{\sin(\theta)}\sum_{n=1}^{N}\left(\frac{R_e}{r}\right)^{n+2}\sum_{m=0}^{n}[-mg^{n,m}\sin(m\phi) + mh^{n,m}\cos(m\phi)]P^{n,m}(\theta). \tag{12}$$

2.1. Dipole model

Expanding Eq. (12) to the first degree and replacing corresponding Legendre functions from Eqs. (6) to (7) yields to the following expression.

$$B_r = 2\left(\frac{R_e}{r}\right)^3\left[g^{1,0}\cos\theta + \left(g^{1,1}\cos\phi + h^{1,1}\sin\phi\right)\sin\theta\right]$$
$$B_\theta = \left(\frac{R_e}{r}\right)^3\left[g^{1,0}\sin\theta - \left(g^{1,1}\cos\phi + h^{1,1}\sin\phi\right)\cos\theta\right].$$
$$B_\phi = \left(\frac{R_e}{r}\right)^3\left[g^{1,1}\sin\phi - h^{1,1}\cos\phi\right] \tag{13}$$

Eq. (13) can be used to model the geomagnetic field as a dipole.

2.2. Centered dipole model

This simplified model uses only the first term of the spherical harmonic expansion to approximate the Earth's magnetic field. This means the magnetic dipole axis is assumed to be aligned with the Earth's rotation axis. The Centered Dipole Model can be obtained from Eq. (14).

$$B_r = 2\left(\frac{R_e}{r}\right)^3 g^{1,0}\cos\theta.$$
$$B_\theta = \left(\frac{R_e}{r}\right)^3 g^{1,0}\sin\theta.$$
$$B_\phi = 0 \tag{14}$$

2.3. Simplified dipole model

Another simple model which is used as a quick tool for approximating geomagnetic field in situations like preliminary design phase can be obtained by simplifying the Dipole Model. A dipole approximation coupled with the assumptions of no Earth rotation and no orbit precession, yields to the following periodic model in orbital frame [12,14].

$$B_x(t) = \frac{\mu_f}{a^3}\cos\omega_o t\ \sin i_m$$
$$B_y(t) = -\frac{\mu_f}{a^3}\cos i_m$$
$$B_z(t) = 2\frac{\mu_f}{a^3}\sin\omega_o t\ \sin i_m, \tag{15}$$

where i_m is the inclination of the spacecraft's orbit respect to the magnetic equator and a is the semi-major axis. The field's dipole strength is $\mu_f = 7.9\times10^{15}\ Wb-m$. Here we use $i_m = i + 11.4^o$ considering the tilt of magnetic equator with respect to geographical equator. As it can be seen in Eq. (15), the geomagnetic field components in this model are simply functions of time rather than latitude and longitude.

Table 1
Gaussian coefficients (nT).

Model	g/h	n	m	2015 Standard	2015 Normalized	Standard SV	Normalized SV	2016 Normalized
Dipole	g	1	0	−29,442	−29,442	10.3	11.4	−29,432
	g	1	1	−1501	−1501	18.1	16.7	−1482.9
	h	1	1	4797.1	4797.1	−26.6	−28.8	4770.5
Quadrupole	g	2	0	−2445.1	−3667.6	−8.7	−13.05	−3680.7
	g	2	1	3012.9	5218.5	−3.3	−5.72	5212.8
	h	2	1	−2845.6	−4928.7	−27.4	−47.46	−4976.2
	g	2	2	1676.7	1452.1	2.1	1.82	1453.9
	h	2	2	−641.9	−555.9	−14.1	−12.21	−568.1
Octupole	g	3	0	1350.7	3376.8	3.4	8.5	3385.3
	g	3	1	−2352.3	−7202.4	−5.5	−16.84	−7219.3
	h	3	1	−115.3	−353.03	8.2	25.11	−327.93
	g	3	2	1225.6	2373.4	−0.7	−1.36	2372
	h	3	2	244.9	474.25	−0.4	−0.77	473.47
	g	3	3	582.0	460.11	−10.1	−7.98	452.13
	h	3	3	−538.4	−425.64	−1.8	−1.42	−427.07

2.4. Quadrupole model

One step further than dipole approximation is to expand the spherical harmonics in Eq. (12) to the second degree ($N = 2$) to include the quadrupolar effects of the geomagnetic field. This yields to the following expression.

$$\begin{aligned}
B_r &= B_r^{Dipole} + 3\left(\frac{R_e}{r}\right)^4\left[\frac{1}{2}g^{2,0}\left(\cos 2\theta + \frac{1}{3}\right) + \frac{1}{2}\left(g^{2,1}\cos\phi + h^{2,1}\sin\phi\right)\sin 2\theta + \frac{1}{2}\left(g^{2,2}\cos 2\phi + h^{2,2}\sin 2\phi\right)(1-\cos 2\theta)\right]\\
B_\theta &= B_\theta^{Dipole} + \left(\frac{R_e}{r}\right)^4\left[g^{2,0}\sin 2\theta + \left(g^{2,1}\cos\phi + h^{2,1}\sin\phi\right)\cos 2\theta - \left(g^{2,2}\cos 2\phi + h^{2,2}\sin 2\phi\right)\sin 2\theta\right]\\
B_\phi &= B_\phi^{Dipole} + \left(\frac{R_e}{r}\right)^4\left[\left(g^{2,1}\sin\phi - h^{2,1}\cos\phi\right)\cos\theta - 2\left(g^{2,2}\sin 2\phi - h^{2,2}\cos 2\phi\right)\sin\theta\right].
\end{aligned} \tag{16}$$

Eq. (16) is the Quadrupole Model of the Earth's magnetic field. It considers the first eight terms of the harmonics and so contains a total number of eight normalized Gaussian coefficients.

2.5. Octupole model

The next model represents the Earth's magnetic field by expanding the spherical harmonics to the third degree ($N = 3$) which corresponds to taking account of the first 15 terms. The Octupole Model is derived in Eq. (17).

$$\begin{aligned}
B_r &= B_r^{Quadrupole} + 4\left(\frac{R_e}{r}\right)^5\left[\frac{1}{2}g^{3,0}\cos\theta\left(\cos 2\theta - \frac{1}{5}\right) + \frac{1}{2}\left(g^{3,1}\cos\phi + h^{3,1}\sin\phi\right)\sin\theta\left(\cos 2\theta - \frac{3}{5}\right)\right.\\
&\quad\left. + \frac{1}{2}\left(g^{3,2}\cos 2\phi + h^{3,2}\sin 2\phi\right)\cos\theta(1-\cos 2\theta) + \frac{1}{2}\left(g^{3,3}\cos 3\phi + h^{3,3}\sin 3\phi\right)\sin\theta(1-\cos 2\theta)\right]\\
B_\theta &= B_\theta^{Quadrupole} - 3\left(\frac{R_e}{r}\right)^5\left[\frac{1}{2}g^{3,0}\sin\theta\left(\cos 2\theta - \frac{3}{5}\right) + \frac{1}{2}\left(g^{3,1}\cos\phi + h^{3,1}\sin\phi\right)\cos\theta\left(\cos 2\theta - \frac{2}{5}\right)\right.\\
&\quad\left. + \frac{1}{2}\left(g^{3,2}\cos 2\phi + h^{3,2}\sin 2\phi\right)\sin\theta\left(\cos 2\theta - \frac{1}{3}\right) + \frac{1}{2}\left(g^{3,3}\cos 3\phi + h^{3,3}\sin 3\phi\right)\cos\theta(1-\cos 2\theta)\right].\\
B_\phi &= B_\phi^{Quadrupole} + \left(\frac{R_e}{r}\right)^5\left[\frac{1}{2}\left(g^{3,1}\sin\phi - h^{3,1}\cos\phi\right)\left(\cos 2\theta + \frac{3}{5}\right) + \left(g^{3,2}\sin 2\phi - h^{3,2}\cos 2\phi\right)\sin 2\theta\right.\\
&\quad\left. + \frac{3}{2}\left(g^{3,3}\sin 3\phi + h^{3,3}\cos 3\phi\right)(1-\cos 2\theta)\right]
\end{aligned} \tag{17}$$

Table 1 contains the Gaussian coefficients from IGRF-12 (2015) required for the Dipole, Quadrupole and Octupole models. All coefficients are first converted to normalized form using Eqs. (9) and (10) then a 1 year shift is applied on the epoch values using Eq. (11) so that they are applicable for 2016.

2.6. Higher order models

In previous sections, the equations for Dipole, Quadrupole and Octupole models were derived and corresponding normalized Gaussian coefficients were given to provide an explicit and convenient tool for approximating the geomagnetic field up to the 3rd degree. However, expanding the harmonics for higher order models leads to very long expressions which

are not desirable. In this case, programming a numerical algorithm for expanding the harmonics and generating desired coefficients from IGRF using provided relations would be much more preferable.

The 4th degree model which in this context is named Sedecimupole Model is obtained by considering the first 24 terms of the spherical harmonics. The maximum spherical harmonic degree of the expansion, N, determines the accuracy of the modeling. However, it should be chosen so that the coefficients of the model are reliably determined given the available coverage and quality of observations. The maximum degree was limited to 10 in previous versions of IGRF but it is now extended to 13 in IGRF-11 and 12 as a result of excellent data provided by Ørsted and CHAMP satellites. Expanding the potential function to the maximum degree of 13 corresponds to taking account of all 195 Gaussian coefficients provided by IGRF-12.

In this study, the 13th degree model is named Reference Model and is used in the simulations to evaluate the accuracy of lower degree models.

3. Transformation of the earth's magnetic field from local tangent plane coordinate to body frame

The magnetic field literature normally refers to three components consisting of North, East and Down (nadir relative to the Earth). The spherical coordinates (r, θ, φ) which is called local tangent plane coordinate system is very similar to NED (North-East-Down) coordinates. These components are obtained from Eq. (18) [8].

$$\begin{aligned} B_N &= -B_\theta \cos\varepsilon - B_r \sin\varepsilon \\ B_E &= B_\phi \\ B_D &= B_\theta \sin\varepsilon - B_r \cos\varepsilon, \end{aligned} \tag{18}$$

where $\varepsilon \equiv \lambda - \delta < 0.2^o$, λ is the geodetic latitude and $\delta \equiv 90 - lat$ is the declination.

In order to use the Earth's magnetic field in attitude control applications, the field in spacecraft body frame is needed, see Eq. (2). As the first step, the Earth's magnetic field in local tangent plane coordinates is transformed to the fixed Earth inertial coordinates utilizing Eq. (19).

$$\begin{aligned} B_x^I &= (B_r \cos\delta + B_\theta \sin\delta)\cos\alpha - B_\phi \sin\alpha \\ B_y^I &= (B_r \cos\delta + B_\theta \sin\delta)\sin\alpha + B_\phi \cos\alpha \\ B_z^I &= B_r \sin\delta - B_\theta \cos\delta \\ \delta &= 90 - colat, \alpha = long + \theta_g, \end{aligned} \tag{19}$$

where B_x^I, B_y^I and B_z^I are geomagnetic field components in inertial coordinates. δ and θ_g indicate declination and celestial time in Greenwich.

The next step is to transform the magnetic field to the orbital frame using Eq. (20).

$$\begin{aligned} B_x^O &= (-\mathrm{s}\,\Theta \mathrm{c}\,\Omega - \mathrm{c}\,\Omega\,\mathrm{c}\,i\,\mathrm{s}\,\Omega)(B_r \mathrm{c}\delta \mathrm{c}\alpha + B_\theta \mathrm{s}\delta \mathrm{c}\alpha - B_\phi \mathrm{s}\alpha) + (-\mathrm{s}\,\Theta\,\mathrm{s}\,\Omega + \mathrm{c}\,\Theta\,\mathrm{c}\,i\,\mathrm{c}\,\Omega)(B_r \mathrm{c}\delta \mathrm{s}\alpha + B_\theta \mathrm{s}\delta \mathrm{s}\alpha + B_\phi \mathrm{c}\alpha) \\ &\quad + \mathrm{c}\,\Theta\,\mathrm{s}\,i(B_r \mathrm{s}\delta - B_\theta \mathrm{c}\delta) \\ B_y^O &= (-si\,\mathrm{s}\,\Omega)(B_r \mathrm{c}\delta \mathrm{c}\alpha + B_\theta \mathrm{s}\delta \mathrm{c}\alpha - B_\phi \mathrm{s}\alpha) + (si\,\mathrm{c}\,\Omega)(B_r \mathrm{c}\delta \mathrm{s}\alpha + B_\theta \mathrm{s}\delta \mathrm{s}\alpha + B_\phi \mathrm{c}\alpha) - \mathrm{c}i(B_r \mathrm{s}\delta - B_\theta \mathrm{c}\delta) \\ B_z^O &= (-\mathrm{c}\,\Theta\,\mathrm{c}\,\Omega + \mathrm{s}\,\Theta\,\mathrm{c}i\,\mathrm{s}\Omega)(B_r \mathrm{c}\delta \mathrm{c}\alpha + B_\theta \mathrm{s}\delta \mathrm{c}\alpha - B_\phi \mathrm{s}\alpha) + (-\mathrm{c}\Theta\,\mathrm{s}\Omega - \mathrm{s}\Theta\,\mathrm{c}i\,\mathrm{c}\Omega)(B_r \mathrm{c}\delta \mathrm{s}\alpha + B_\theta \mathrm{s}\delta \mathrm{s}\alpha + B_\phi \mathrm{c}\alpha) \\ &\quad - \mathrm{s}\Theta\,si(B_r \mathrm{s}\delta - B_\theta \mathrm{c}\delta), \end{aligned} \tag{20}$$

Θ, Ω and i are the orbital parameters. Θ is true anomaly, Ω and i show the right ascension of the ascending node and inclination respectively. sand c denote sine and cosine functions.

Finally, transforming the magnetic field to the satellite body frame would be as Eq. (21).

$$\begin{aligned} B_{NLx}^B &= \mathrm{c}\psi\,\mathrm{c}\theta B_x^O + (\mathrm{c}\psi\,\mathrm{s}\theta\mathrm{s}\phi - \mathrm{s}\psi\,\mathrm{c}\phi)B_y^O + (\mathrm{c}\psi\,\mathrm{c}\phi\mathrm{s}\theta + \mathrm{s}\psi\,\mathrm{s}\phi)B_z^O \\ B_{NLy}^B &= \mathrm{s}\psi\,\mathrm{c}\theta B_x^O + (\mathrm{s}\psi\,\mathrm{s}\theta\mathrm{s}\phi + \mathrm{c}\psi\,\mathrm{c}\phi)B_y^O + (\mathrm{s}\psi\,\mathrm{s}\theta\mathrm{c}\phi - \mathrm{c}\psi\,\mathrm{s}\phi)B_z^O, \\ B_{NLz}^B &= -\mathrm{s}\theta B_x^O + \mathrm{c}\theta\mathrm{s}\phi B_y^O + \mathrm{c}\theta\,\mathrm{c}\phi B_z^O \end{aligned} \tag{21}$$

φ, θ, ψ indicate roll, pitch and yaw angles respectively.

Eq. (21) shows the nonlinear matrix transformation from the orbital frame to the body frame. Assuming small Euler angles, the cosine is approximately equal to 1 and the sine is approximated by the value of the angles in radians, the equation is linearized as Eq. (22).

$$\begin{aligned} B_{Lx}^B &= B_x^O - \psi B_y^O + \theta B_z^O \\ B_{Ly}^B &= \psi B_x^O + B_y^O - \phi B_z^O \\ B_{Lz}^B &= -\theta B_x^O + \phi B_y^O + B_z^O. \end{aligned} \tag{22}$$

As it will be shown in Section 4.4, the "small angle" definition is usually too general and its value strongly depends on the desired accuracy of the mission. Therefore, its upper bound value should be investigated in any specific case.

The reference frames introduced in this section are shown in Fig. 1.

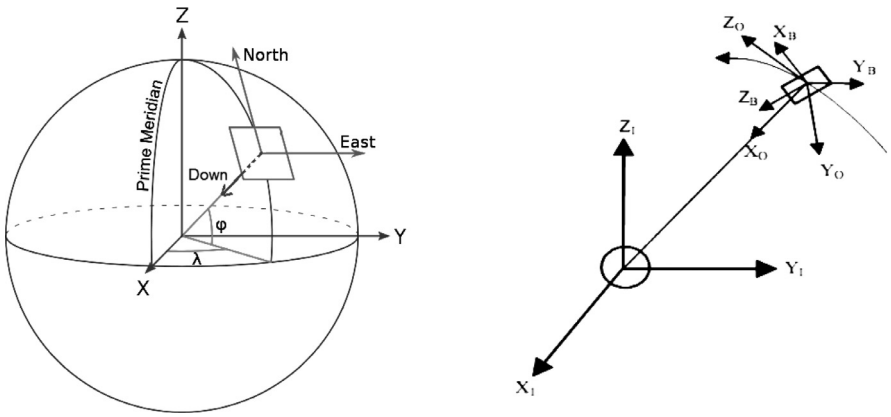

Fig. 1. NED (left), Inertial, Orbital and Body frames (right).

Table 2
Comparison of WMM and our Reference Model results for modeling the Earth's magnetic field.

		WMM results (nT)	Reference model results (nT)	Error (%)
London 0 height	B_{North}	19,450	19,160	1.49
	B_{East}	−386	−391	1.30
	B_{Down}	44,641	44,648	0.02
	$\|B\|$	48,696	48,587	0.22
London 500 km height	B_{North}	15,897	15,680	1.36
	B_{East}	−540	−539.1	0.17
	B_{Down}	35,676	35,697	0.06
	$\|B\|$	39,061	38,992	0.18
0 Lat, Long 0 height	B_{North}	27,576	27,656	0.29
	B_{East}	−2729	−2696	1.21
	B_{Down}	−15,782	−15,889	0.68
	$\|B\|$	31,890	32,009	0.37
0 Lat, Long 500 km height	B_{North}	21,648	21,709	0.28
	B_{East}	−2296	−2278	0.78
	B_{Down}	−10,669	−10,735	0.62
	$\|B\|$	24,243	24,325	0.34

4. Simulations and results

4.1. Reference model verification

A MATLAB code has been developed by the authors in order to model the Earth's magnetic field using the relations presented in previous sections and IGRF-12 coefficients. In the first step, the code results for Reference Model are compared with the World Magnetic Model for verification. WMM is a standard model based on IGRF produced jointly by British Geological Survey and US National Geophysical Data Center. WMM is widely used for navigation and attitude reference systems and is revised every five years [19].

The results from WMM and our Reference Model for two points (London and the intersection of equator and prime meridian i.e. point of zero latitude and longitude) on the Earth surface and on the height of 500 km are presented in Table 2 as North, East and Down components and total intensity of the geomagnetic field. The error of our Reference Model's results compared to WMM is included as well. It should be mentioned that these results are obtained for the year of 2014.

According to Table 2 and more results for other points on the Earth, the accuracy of our Reference Model based on the 12th generation of IGRF coefficients is found satisfactory enough to be employed in the following simulations and comparisons.

4.2. Models comparison

In this section, all discussed models in Section 2 are used to simulate the Earth's magnetic field. They are first transferred to the orbital frame using the provided transformations in Section 3 and then evaluated in different aspects. A circular orbit with semi-major axis of 500 km and inclination of 60° is considered for first group of simulations.

Figs. 2 and 3 illustrate the *x,y* and *z* components of the Earth's magnetic field and the intensity of the field for all models respectively.

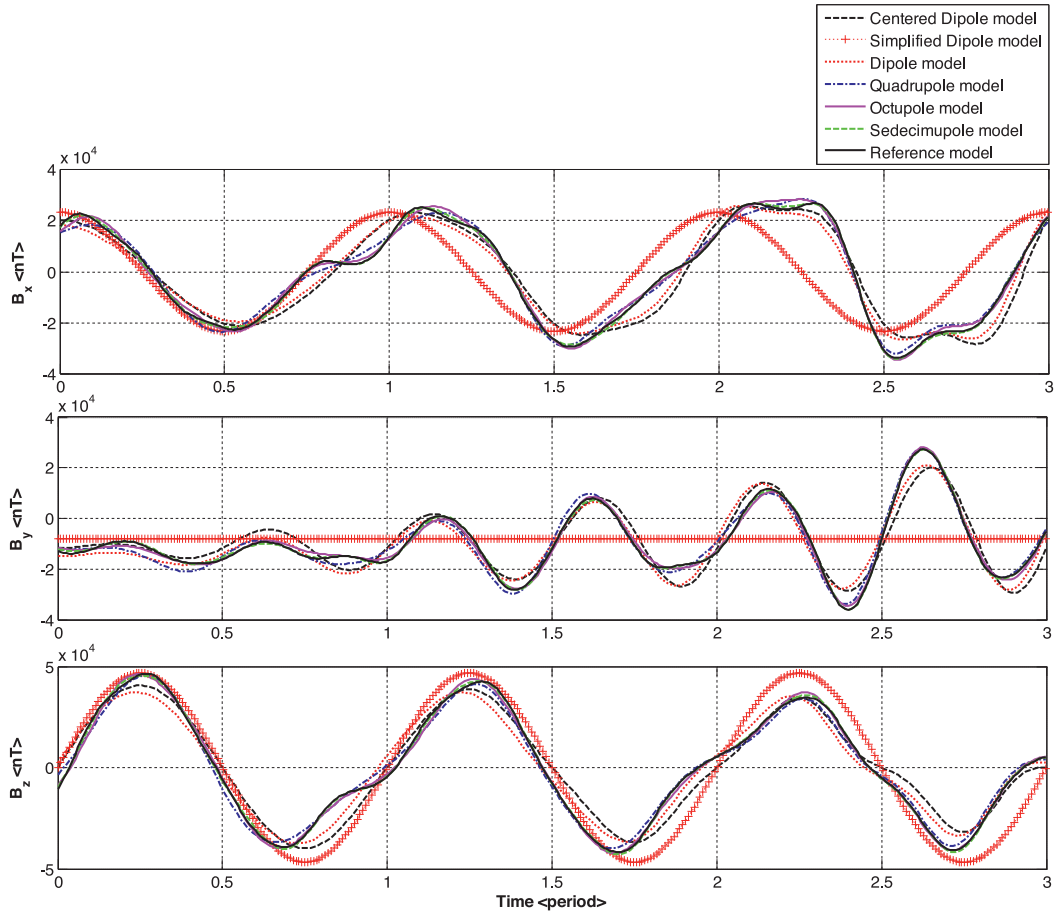

Fig. 2. *x*, *y* and *z* components of geomagnetic field for all models in orbital frame.

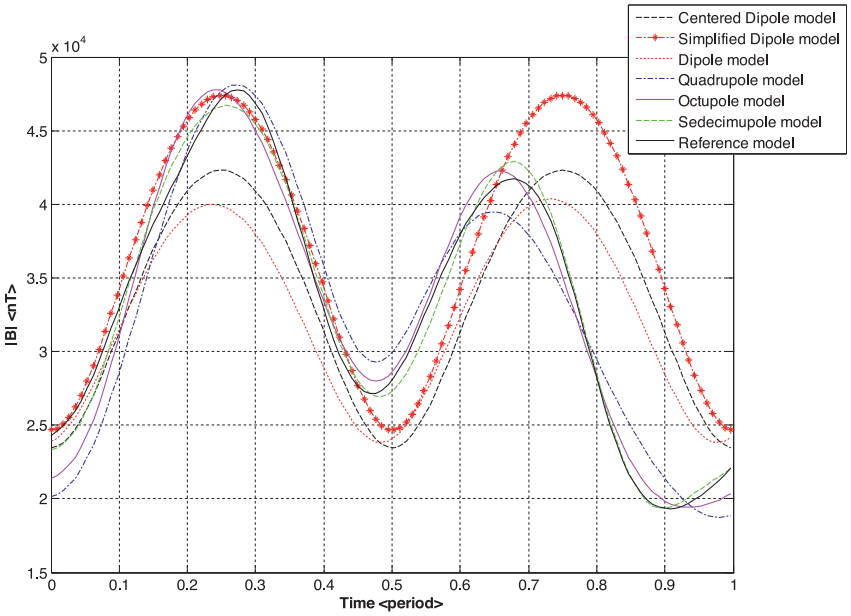

Fig. 3. Intensity of geomagnetic field for all models.

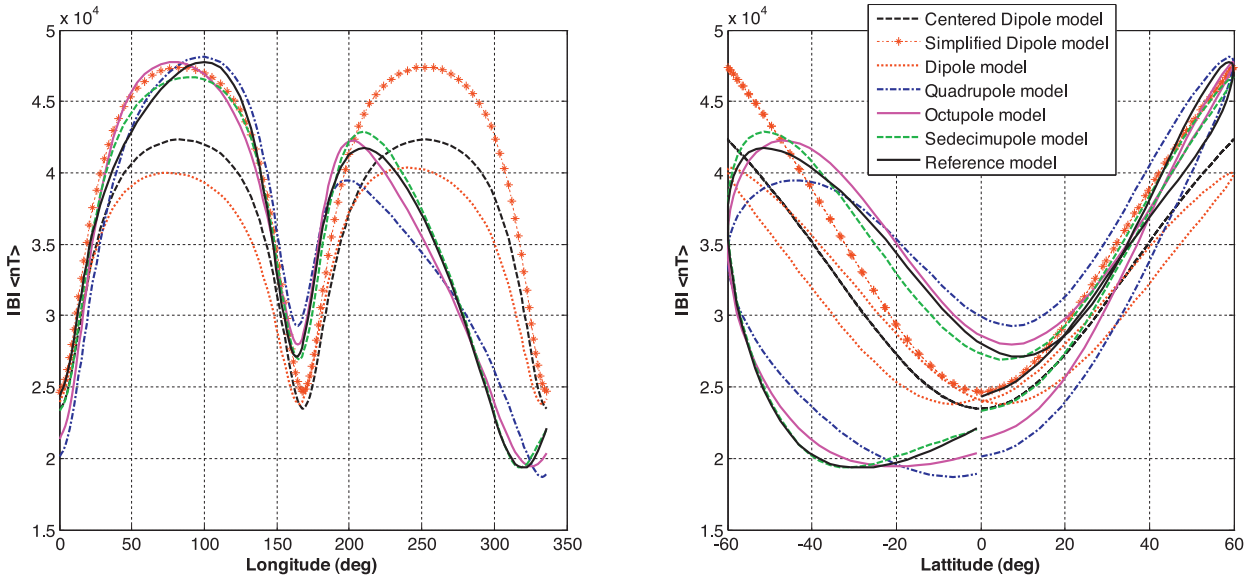

Fig. 4. Intensity of geomagnetic field against longitude and latitude on the Earth.

According to Fig. 2, it can be seen that the Simplified Dipole Model (SDM) is the least accurate model in tracking the Reference Model. Particularly, this model is not able to simulate the oscillations in y direction and only gives a constant average. From Fig. 3, the Centered Dipole Model is shown to be a better approximate of the Dipole Model rather than the SDM. The accuracy of the other models has improved as the expansion order of modeling is increased.

In Fig. 4, the Earth's magnetic field intensity obtained from mentioned models is plotted against the Earth's latitude and longitude. This figure corresponds to almost one orbital period around the Earth. Some interesting observations can be made here. Intensity of the field tends to decrease from poles to the equator. Also, lower degree models produce less accurate results as the intensity increases toward Earth's poles.

The relative error of the models during one orbital period is shown in Fig. 5 for inclinations of 0°, 60° and 90°.

As it can be seen, less accurate models which are Simplified Dipole, Centered Dipole, Dipole and Quadrupole Models have experienced some noticeable errors. The models error trend is similar for orbits with 60° and 90° of inclination with a maximum error of 92% and 82% respectively for SD model. However, all models were more accurate in equatorial orbit.

This evident effect of orbital inclination on the accuracy of the models leads us to a thorough analysis presented in the next section.

4.3. Inclination and altitude effects

Several simulations are performed here to investigate the effects of inclination and altitude on the accuracy of the geomagnetic models.

In an inclined low Earth orbit, the Earth's rotation causes a change in geomagnetic field that satellite is exposed to in every orbit. However, this is an almost periodic effect. In order to take account of these periodic changes, simulations are extended to 20 to 30 orbital periods around the Earth. Fig. 6 illustrates the results for models relative errors in an orbit with $i = 60°$. Average error of models for modeling the intensity of geomagnetic field during 30 orbital periods is determined for varying the orbital inclination from 0° to 180° and results are illustrated in Fig. 7.

As it can be seen, lower order models namely SDM, CDM and DM were most accurate at the low end and high end of the inclination range i.e. near 0° and 180° respectively, with an average error of about 10% to 12% at these points. These three 1st degree models also experienced a local minimum error near the polar area and two maximum errors in the mid-range of equator and pole. The 2nd and 3rd degree models (QM and OM) exhibit an average error of about 9% and 4% respectively. The 4th degree model (SM) is the most accurate one with an average error less than 2 percent. Another observation can be made here that as the degree of modeling is increased, the inclination effects on the accuracy of models become negligible.

Table 3 summarizes the accuracy of the models in above simulations expressed as maximum and average errors. This comparison is performed with respect to Reference Model for various inclinations at an orbital height of 500 km and 30 orbital periods.

The effect of altitude on Earth's magnetic field models is illustrated in Fig. 8. As expected, it can be seen that by increasing altitude from Earth surface, the intensity of magnetic field drastically decreases. This effect is most noticeable in low Earth orbits. According to Fig. 9, models lower than fourth degree experience a significant inaccuracy in such orbits.

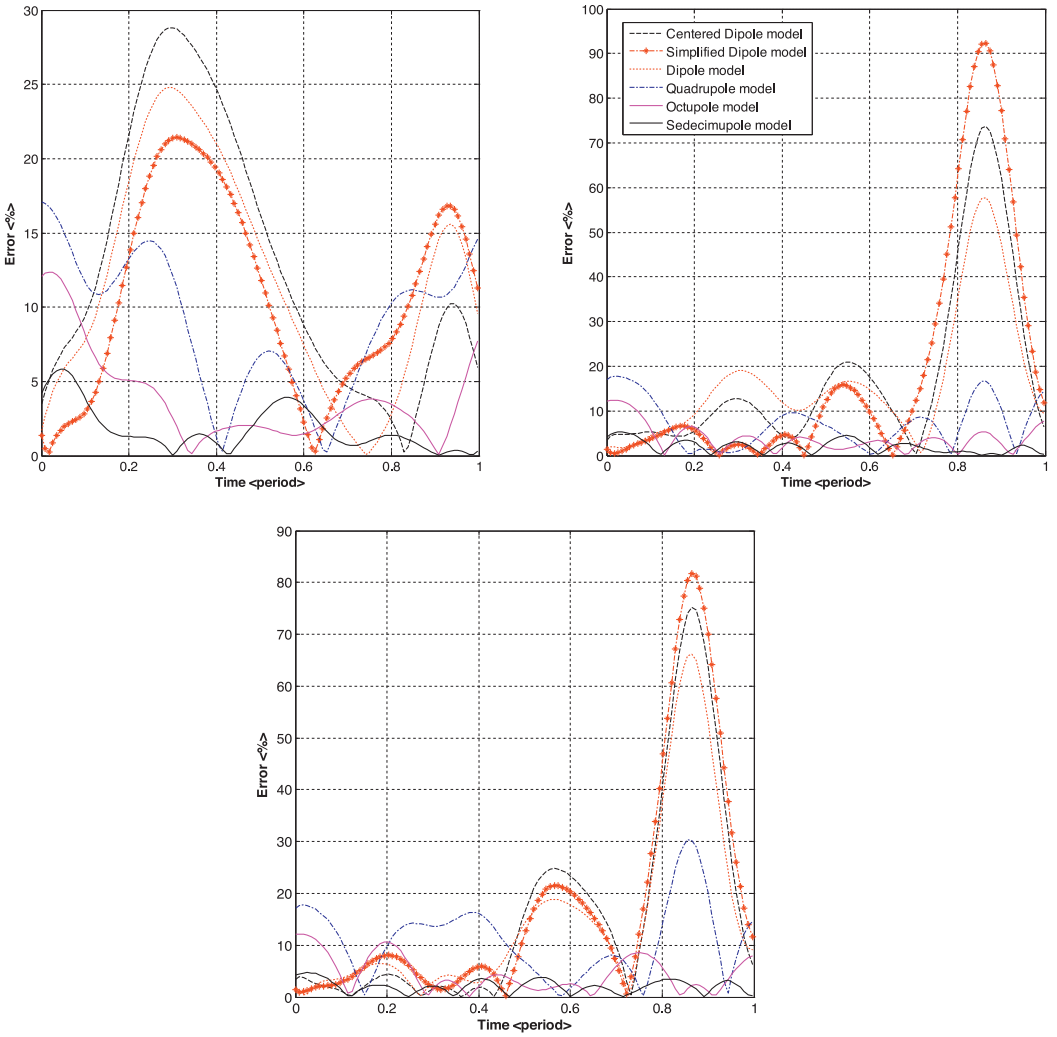

Fig. 5. Relative error of all models for inclinations of $i = 0°$ (top left), $i = 60°$ (top right) and $i = 90°$ (down).

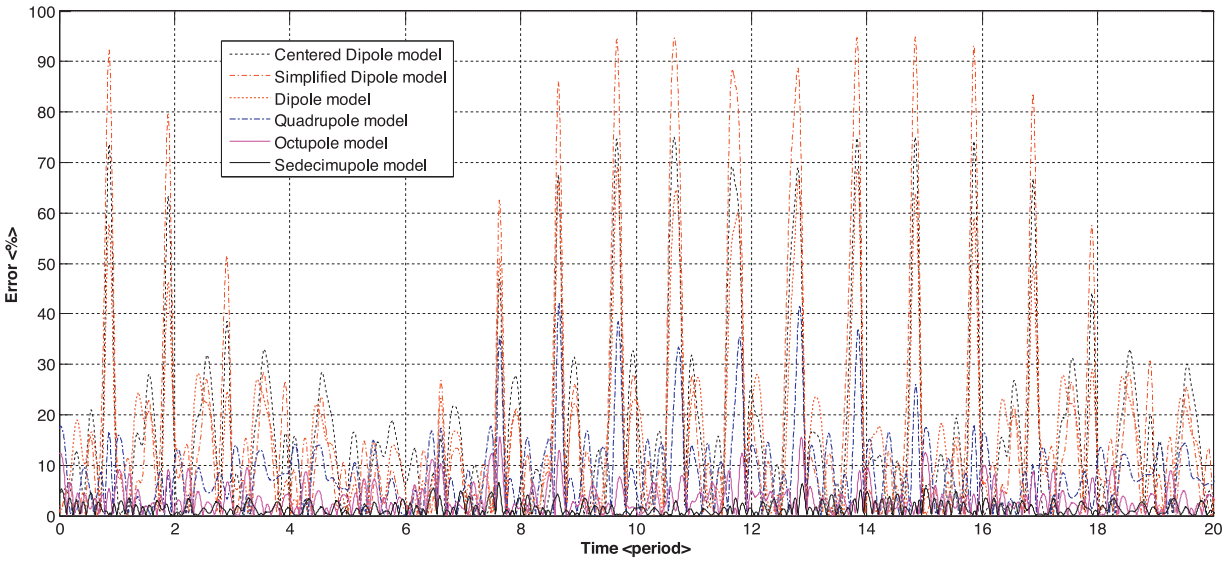

Fig. 6. Models relative error of geomagnetic field intensity in 30 orbits with $i = 60°$.

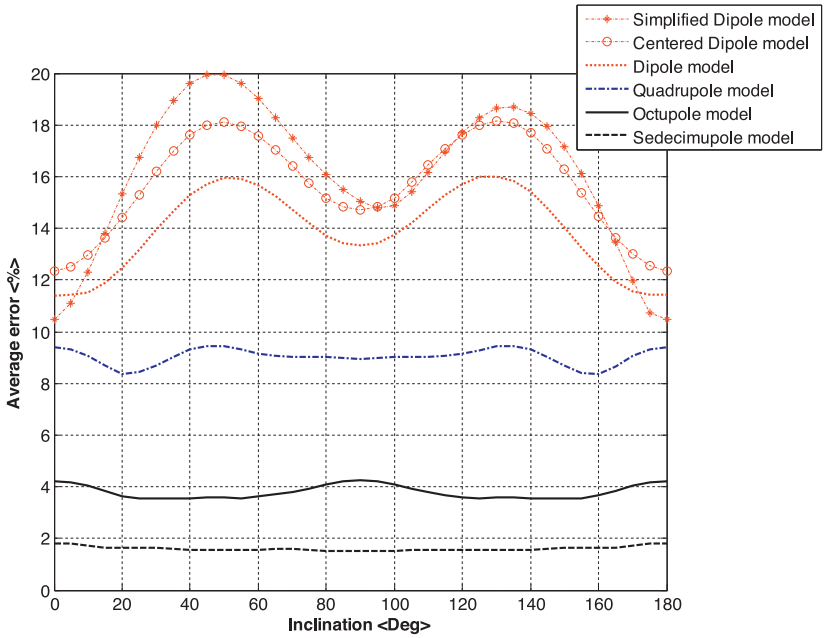

Fig. 7. Models average error of geomagnetic field intensity against inclination in 30 orbits.

Table 3
Summary of models error (average and maximum) regarding the inclination change.

	Average error (%)						Maximum error (%)					
Inclination (Deg)	SD model	CD model	D model	Q model	O model	S model	SD model	CD model	D model	Q model	O model	S model
0	10.6	12.4	11.5	9.4	4.2	1.8	25.2	28.9	25	17.2	12.3	5.8
10	12.5	13.0	11.6	9.1	4.0	1.7	49.9	32.2	26.4	17.8	12.4	5.9
20	15.5	14.5	12.6	8.4	3.6	1.6	78	46.2	34.3	17.8	12.4	5.9
30	18.1	16.3	14.1	8.7	3.5	1.6	98.4	64.3	48.2	25.4	12.4	5.9
40	19.8	17.7	15.4	9.4	3.5	1.6	105	74.1	61.8	38.6	15.5	6.6
50	20.1	18.2	16.1	9.5	3.6	1.6	103	76	69.8	42.3	15.4	6.4
60	19.2	17.7	15.8	9.2	3.6	1.6	95.9	75.7	69.8	41.6	14.9	6.5
70	17.6	16.5	14.8	9.1	3.8	1.6	91.1	76.1	69.9	42.3	15.1	6.5
80	16.2	15.3	13.8	9.1	4.1	1.5	86.3	75.5	69.6	41	14.8	6.6
90	15.2	14.8	13.5	9	4.2	1.5	82.4	75.7	67.3	40.6	14.8	6.6

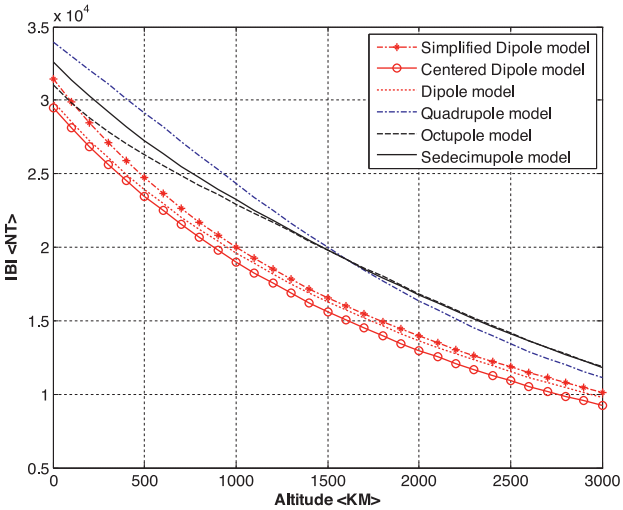

Fig. 8. Geomagnetic field intensity for all models against altitude.

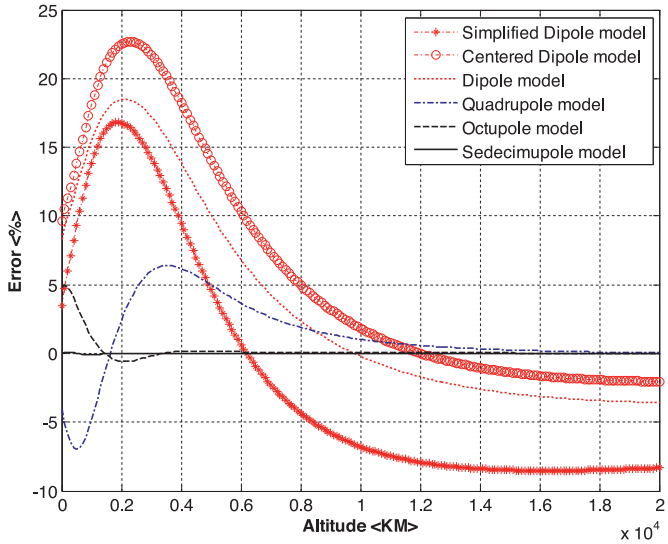

Fig. 9. Geomagnetic field intensity error for all models against altitude.

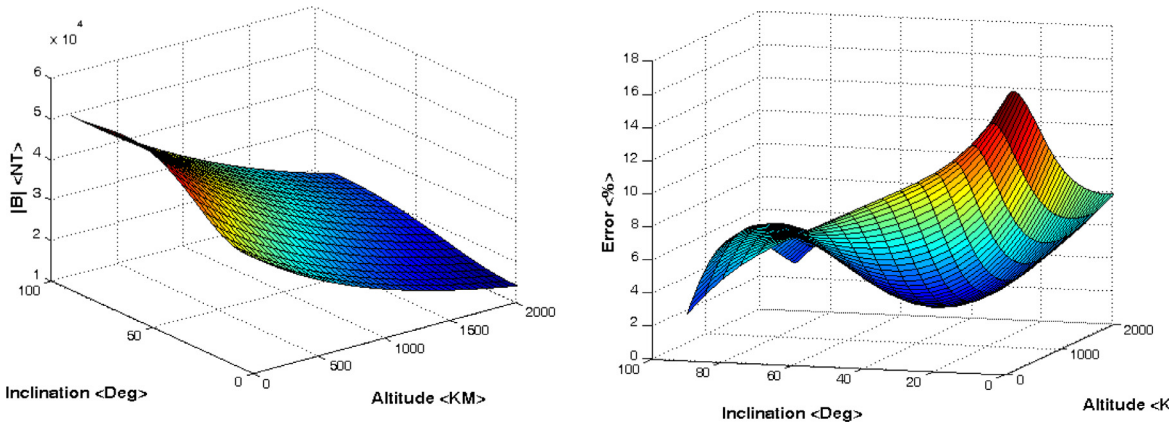

Fig. 10. Geomagnetic field intensity of Reference Model (left) and error of Simplified Dipole Model (right) against altitude and inclination for 1/5 of orbital time.

For an orbital altitude of 500 km, the QM and SDM experience a 5% error while the DM and CDM show 10% and 15% of error respectively. As the Earth's magnetic field gets weaker in higher altitudes, models' intensity and error decreases.

Effects of altitude and inclination were studied in previous simulations. Here, additional simulations are performed in order to observe these effects simultaneously. An inclination change from equatorial to polar and altitude range up to 2000 km for low Earth orbits are considered. It should be mentioned that the following results are obtained for specified times of the orbital motion. Results for intensity of the field obtained from the Reference Model and the error of the Simplified Dipole Model are plotted as three-dimensional surfaces in Figs. 10–12.

As it can be seen in Fig. 10, the intensity of the field is increased as we move from the Earth's equator toward the poles and it decreases by elevating to higher orbits at the time of 1/5 of the orbital period. By observing the combination of the changes for both parameters, it is shown that the inclination effects are more intense in lower orbits. Analyzing the results of error simulation indicates that the Simplified Dipole Model error follows a third-order curve in altitudes less than 400 km with the maximum at equator and the minimum at polar area. In higher orbits, the error behavior follows a fourth-order curve. The minimum occurs at about inclination of 40° and altitude of 1500 km while the maximum error remains at equator.

By advancing in the orbit to 2/5 of the period, according to Fig. 11, geomagnetic field has changed its behavior regarding the inclination as opposed to previous simulation. Here, for orbits under 1000 km, the field is at maximum intensity for equatorial inclinations. From 1000 to 2000 km the opposite holds, meaning the maximum intensity occurs at polar inclinations. Error of the SD model in this simulation shows a distinct maximum at very low orbits with near polar inclinations, but it reaches a smooth surface in orbits higher than 500 km which is not very sensitive to inclination changes.

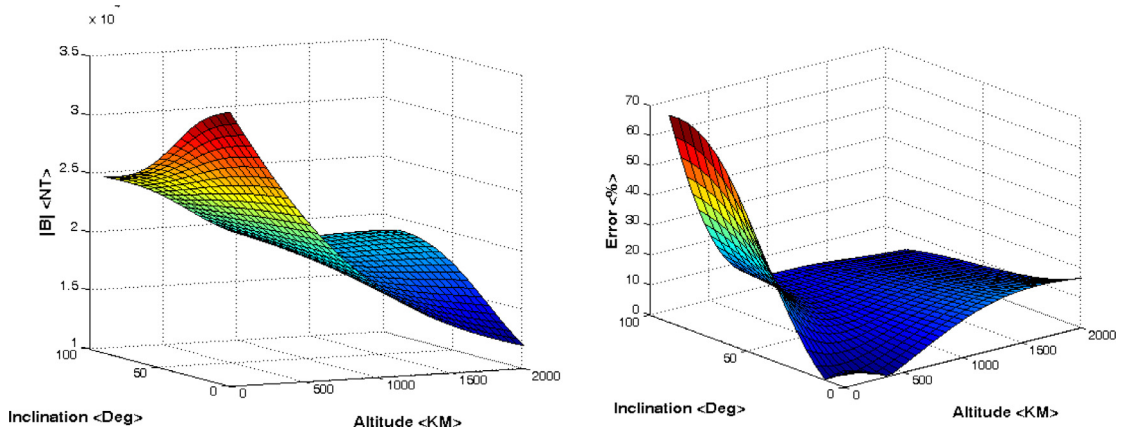

Fig. 11. Geomagnetic field intensity of Reference Model (left) and error of Simplified Dipole Model (right) against altitude and inclination for 2/5 of orbital time.

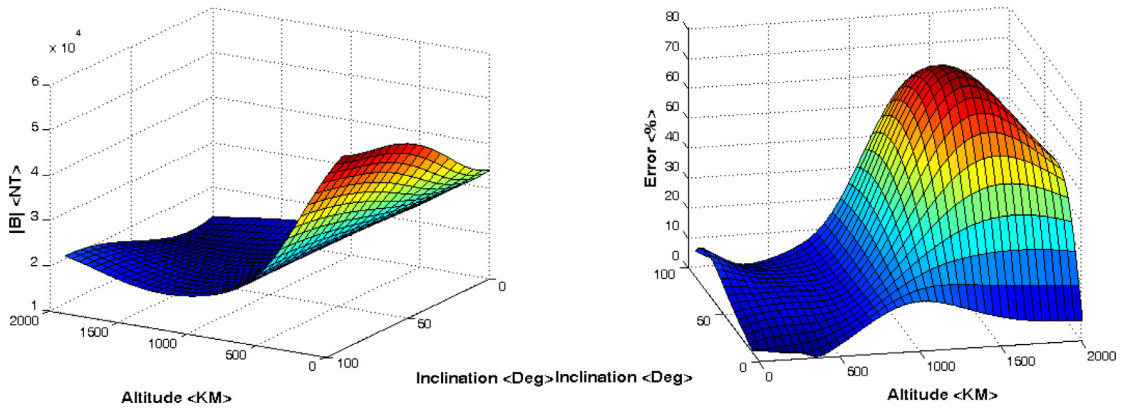

Fig. 12. Geomagnetic field intensity of Reference Model (left) and error of Simplified Dipole Model (right) against altitude and inclination for 4/5 of orbital time.

Moving to the last one fifth point of the period as shown in Fig. 12, the geomagnetic field intensity is almost identical to the first one fifth point of the orbit shown in Fig. 10, with only a difference of being a concave surface rather than a convex one. The SD model error is reversed in terms of convexity as well. The maximum error of 75% occurs at around altitude of 1500 km and inclination of 55°. This model experiences a significant error growth for altitudes higher than 800 km except for near equatorial inclinations.

4.4. Linear and nonlinear transformations

In the next step, the Earth's magnetic field is simulated in the body frame of the spacecraft. According to Eqs. (19) and (20), there are two transformations (Linear and Nonlinear) in order to transform the magnetic field from orbital frame to body frame. The linearization is performed assuming small attitude angles. The aim of this section is to investigate the accuracy of linear transformation in order to exactly define the "small angle" term.

The following simulations are performed for an attitude angle range from 0° to 30° in order to study the diverging nature of the linear transformation. The three Euler angles are considered equal to each other in each step of simulation. One orbital period of an equatorial orbit with height of 500 km is considered. The results of geomagnetic field intensity from the Reference Model are illustrated in Fig. 13. While the field modeled with nonlinear transformation is not affected by attitude angles, the linear one is clearly diverging from the original path.

The following dimensionless index is adopted as the modeling error for further investigations.

$$\epsilon = \frac{1}{k}\sum_{j=1}^{k}\frac{\left|B^{NL}_{Roll/Pitch/Yaw} - B^{L}_{Roll/Pitch/Yaw}\right|}{\left|B^{NL}_{Roll/Pitch/Yaw}\right|} \times 100, \tag{23}$$

where NL and L denote using of nonlinear and linear transformations respectively and k is the number of steps in the simulation. The error index for this simulation is calculated and shown in Fig. 14.

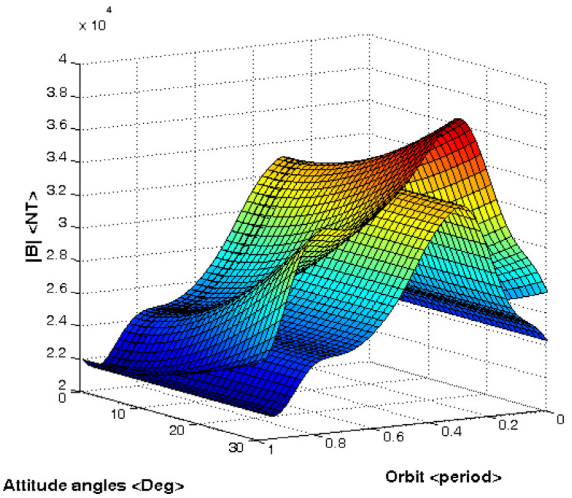

Fig. 13. The divergence of geomagnetic field using linear transformation.

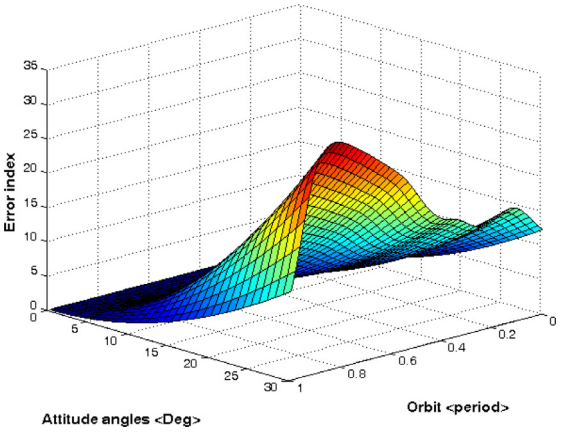

Fig. 14. The error index of geomagnetic field using linear transformation during one period regarding attitude angles.

Table 4
The error index of geomagnetic field components obtained by linear transformation.

	Average error index (%)				Maximum error index (%)			
Attitude angle (Deg)	Roll	Pitch	Yaw	Total	Roll	Pitch	Yaw	Total
1	0.03	0.03	0.02	0.03	0.05	0.04	0.03	0.04
5	0.9	0.7	0.5	0.7	2.2	0.9	0.7	1.1
10	16.2	2.6	2.1	2.7	273	3.2	2.7	4.2
15	4.7	5.2	4.7	6	8	6.8	5.9	9.1
20	9.1	8.4	8.3	10.4	15.1	11.1	10.3	15.7
25	15.6	11.7	12.9	15.7	25.5	15.9	15.8	23.7
30	24.3	14.7	18.3	22	40.4	20.6	22.3	32.8

As it can be seen, the rate of divergence is increased as the attitude angles are increased. A maximum error of about 33% is observed near the end of the orbit. Although it was an equatorial orbit, but more simulation showed that maximum errors experienced for other inclinations are in the same order.

The error index on *x, y* and *z* directions of spacecraft body frame which correspond to roll, pitch and yaw motions respectively, along with the total error of geomagnetic field intensity are presented in Table 4. Results are divided to two parts, maximum and average taken through an orbit.

It was shown that the error index of linear transformation has a rising tendency regarding the increase in attitude angles. According to the results of Table 4, it is now possible to determine the border of validity of the linear transformation for this mission based on the desired accuracy. Based on Figs. 13, 14 and Table 4, it is clear that if for instance, the acceptable average error for the mission is defined about 10% in each direction, the upper limit of the attitude angle to be

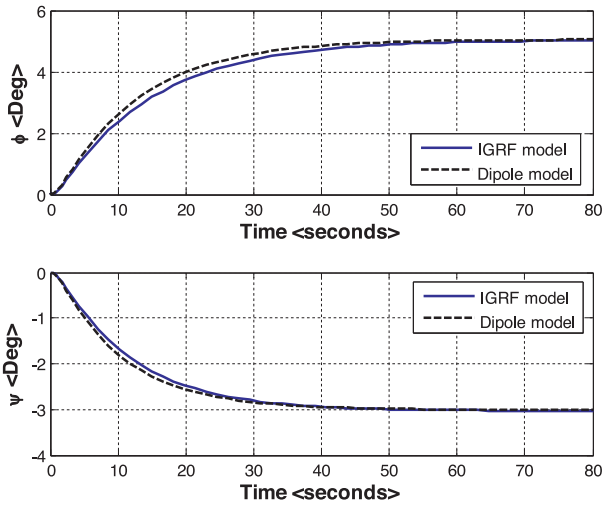

Fig. 15. Roll and yaw responses to step commands for IGRF and Dipole models.

used in linear transformation is about 20° on roll axis, 22° on pitch axis and 21° on yaw axis. While if the maximum error is considered, the upper limits would be 16°, 18° and 19° respectively. In this way, it is possible to find the upper bound of the "small angle" definition for any specific case. It should be mentioned that the validity of the "small angle" depends on the orbit properties and the defined acceptable error for any case.

4.5. Control effort analysis for attitude control application

This section is aimed to demonstrate the effects of geomagnetic field modeling on the accuracy of spacecraft attitude control system. In this regard, an attitude control maneuver is simulated for a satellite in a circular sun-synchronous orbit of 500 km. Satellite's moments of inertia are assumed to be $I_x = 30$, $I_y = 40$, $I_z = 20$ kg.m^2. Two magnetic torqrods are aligned with the X and Z axes of the spacecraft body frame and one reaction wheel is aligned with the Y axis. This configuration is used to prevent the singularity problems in inverting the magnetic field matrix B in Eq. (2).

A PD controller with transfer function of the form $C = P[1 + D\frac{Ns}{s+N}]$ is implemented on the system where proportional gain, derivative gain and filter coefficient are designed to be $P_x = 0.001$, $D_x = 2000$, $N_x = 1$ and $P_y = 0.0015$, $D_y = 1100$, $N_y = 1$ for X and Y axes respectively for a slow response consistent with the magnetic control.

A MATLAB Simulink model was developed for this simulation using nonlinear equations of attitude dynamics. Three closed loop control systems are simultaneously simulated in this model all using the same controllers and reference attitude commands. The first system is developed to design the closed loop control law, without taking account of actuator type. The three-axis controller designed in this system is also used in the other two systems. Second system has the same structure of the first system with the difference that it generates dipole magnetic moments based on the controllers' outputs and applies the corresponding torques on the system in closed loop. The third system is similar to the second one with only difference that it utilizes the accurate IGRF magnetic field model (Reference Model) instead of simplified Dipole Model.

It should be noted that in order to generate the magnetic control torques, first the magnetic moment M is calculated based on inverse of Eq. (2) for a configuration of two torqrods and one reaction wheel [12]:

$$\begin{bmatrix} M_x \\ \dot{h}_{wy} \\ M_z \end{bmatrix} = \frac{1}{B_y^2} \begin{bmatrix} 0 & 0 & B_y \\ B_x B_y & B_y^2 & B_y B_z \\ -B_y & 0 & 0 \end{bmatrix} \begin{bmatrix} T_{cx} \\ T_{cy} \\ T_{cz} \end{bmatrix}. \tag{24}$$

The required magnetic moments are calculated given the control law outputs and the Earth's magnetic field components that the spacecraft is exposed to. Clearly, the modeling accuracy of the geomagnetic field will affect the generated magnetic moments in the spacecraft actuators. To illustrate this effect, the generated magnetic moments are again converted to their actual generated torques using Eq. (2) in which the real geomagnetic field (Reference Model) is used.

In this fashion, a simulation of an attitude control maneuver is performed to evaluate the performance of the control system in which Dipole Model is implemented. The results for following Euler angle command inputs of $\varphi = 5°$ and $\psi = -3°$ are illustrated in Fig. 15.

As it can be seen, both systems properly converge to the aimed target. However, the response of the magnetic control system in which the simpler Dipole Model was used slightly deviates from the system in which the Reference Model was implemented. Although this deviation might seem negligible, more investigation on the consumed energy opposes this statement. Fig. 16 illustrates the summation of control effort corresponding to the total time of this maneuver. In this

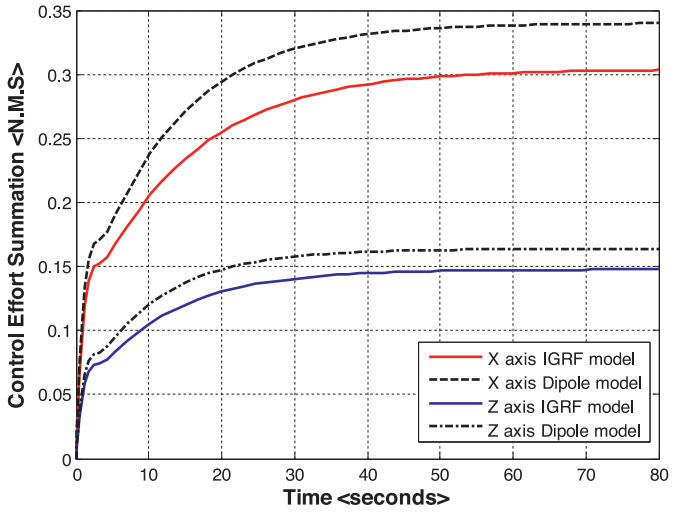

Fig. 16. Control effort summation for roll and yaw axes using IGRF and Dipole models.

figure, the curves have converged to the numbers which are corresponding to the angular impulse or change in angular momentum required for this maneuver.

An increase of about 15% in sum of control effort is observed as a result of modeling the Earth's magnetic field by Dipole Model. This imposed additional energy consumption for such a small angle and short time maneuver definitely demands for long term considerations and possibly could affect the mission life time significantly.

5. Conclusion

Utilizing magnetic torque for spacecraft attitude control is a common way since the actuator is light, inexpensive and relatively easy to use. The contribution of this paper was to simulate the Earth's magnetic field precisely to study the accuracy of some common approximate models under the influence of important parameters such as inclination and altitude. In this study, the 12th generation of IGRF coefficients was used to simulate the Earth's magnetic field, and the results were verified with a standard reference. To compare the trend of accuracy of different models with different orders, the simulation in orbital frame was performed for Simplified Dipole, Centered Dipole, Dipole, Quarupole, Octupole, Sedecimupole and Reference Models and the results were presented and discussed for several scenarios. Despite the improved accuracy of higher order models, it should be noted that the required computational time increases for such models. Hence, the choice of proper model not only needs the knowledge provided by simulation results but also a trade-off between the accuracy and computational effort. In the next step, the Earth's magnetic field was transformed into the body coordinates of the spacecraft in order to be used in attitude control problems. Both linear and nonlinear transformations were simulated and the validity of linear transformation was investigated regarding various attitude angles. The final part of this paper presented the results of a space attitude control maneuver to prove the significant effects of the geomagnetic field modeling on the accuracy and control costs of such mission. Simulation results showed a 15% more control effort in a small angle attitude maneuver when using Dipole Model. While the outcome of this part could make it possible to exactly define the "small angle" term for that specific case, it should be noted that similar simulations might be needed for different scenarios since the results also depend on mission specifications. In conclusion, once the effects of inclination, altitude, latitude and longitude, different attitude angles and other important parameters on the accuracy of geomagnetic field models are well understood, one may be able to choose the appropriate model or transformation according to the mission requirements and desired accuracy of the attitude control system.

References

[1] A.V. Doroshin, M.M. Krikunov, Attitude dynamics of a spacecraft with variable structure at presence of harmonic perturbations, Appl. Math. Model. 38 (Issues 7–8) (2014) 2073–2089.
[2] M. Navabi, Mohammad Radaei, Attitude adaptive control of space systems, in: 6th International Conference on Recent Advances in Space Technologies (RAST2013), Istanbul, Turkey, IEEE, 2013, pp. 973–977.
[3] M. Navabi, H. Rangraz, Comparing optimum operation of Pulse Width-Pulse Frequency and Pseudo-Rate modulators in spacecraft attitude control subsystem employing thruster, in: 6th International Conference on Recent Advances in Space Technologies (RAST2013), Istanbul, Turkey, IEEE, 2013, pp. 625–630.
[4] F. Celani, Robust three-axis attitude stabilization for inertial pointing spacecraft using magnetorquers, Acta Astronaut. 107 (2015) 87–96.
[5] G. Avanzini, E.L. de Angelis, F. Giulietti, Spin-axis pointing of a magnetically actuated spacecraft, Acta Astronaut. 94 (Issue 1) (2014) 493–501.
[6] M.Y. Ovchinnikov, D.S. Roldugin, V.I. Penkov, Three-axis active magnetic attitude control asymptotical study, Acta Astronaut 110 (2015) 279–286.
[7] E. Silani, M. Lovera, Magnetic spacecraft attitude control: a survey and some new results, Control Eng. Pract. 13 (3) (2005) 357–371.
[8] M. Shigehara, Geomagnetic attitude control of an axisymmetric spinning satellite, J. Spacecr. Rockets 9 (6) (June 1972) 391–398.

[9] M.L. Psiaki, Magnetic torque attitude control via asymptotic periodic linear quadratic regulation, J. Guidance, Control, Dyn. 24 (2) (March-April 2001).
[10] R. Wisniewski, Linear time-varying approach to satellite attitude control using only electromagnetic actuation, J. Guidance, Control Dyn. 23 (4) (2000) 640–646.
[11] M. Navabi, N. Nasiri, Simulating the earth magnetic field according to the 10 th generation of IGRF coefficients for spacecraft attitude control applications, in: 5th International Conference on Recent Advances in Space Technologies (RAST2011), Istanbul, Turkey, IEEE, 2011, pp. 584–588.
[12] R. Hurtado-Velasco, J. Gonzalez-Llorente, Simulation of the magnetic field generated by square shape Helmholtz coils, Appl. Math. Model. 40 (23-24) (2016) 9835–9847.
[13] M. Navabi and N. Nasiri, Three-axis stabilization of a low earth orbit spacecraft utilizing three magnetorquers and reaction wheels combinations, according to energy consumption, 61st International Astronautical Congress, Prague, Czech Republic, 2010.
[14] J.R. Wertz, Spacecraft Attitude Determination and Control, KLUWER academic publisher, 1997.
[15] Thebault, et al., International geomagnetic reference field: the 12th generation, Earth, Planets Sp. 67 (2015) 79.
[16] M. Navabi, N. Nasiri, M. Dehghan, Modeling and numerical simulation of linear and nonlinear spacecraft attitude dynamics and gravity gradient moments: a comparative study, Commun. Nonlinear Sci. Numer. Simul. 17 (2) (Feb. 2012) 1065–1084.
[17] M.J. Sidi, Spacecraft dynamics and control, A Practical Engineering Approach, Cambridge University Press, 1997.
[18] N. Olsen, C. Stole, Satellite geomagnetism, Annu. Rev. Earth Planet. Sci. 40 (2012) 441–465.
[19] World Magnetic Model, 2015, visited at 2015. http://www.geomag.bgs.ac.uk/data_service/models_compass/wmm_calc.html.